MAGNETIC RESONANCE IN CHEMISTRY
Magn. Reson. Chem. 2004; **42**: 218–230
Published online in Wiley InterScience (www.interscience.wiley.com). DOI: 10.1002/mrc.1325

MRC

Site-directed ^{13}C solid-state NMR studies on membrane proteins: strategy and goals toward revealing conformation and dynamics as illustrated for bacteriorhodopsin labeled with [1-^{13}C]amino acid residues

Hazime Saitô,* Jun Mikami, Satoru Yamaguchi, Michikazu Tanio, Atushi Kira, Tadashi Arakawa, Kazutoshi Yamamoto and Satoru Tuzi

Department of Life Science, Graduate School of Science, Himeji Institute of Technology, Harima Science Garden City, Kamigori, Hyogo 678-1297, Japan

Received 17 March 2003; Revised 2 August 2003; Accepted 20 August 2003

We have so far demonstrated that well-resolved and site-specifically assigned ^{13}C peaks as recorded by site-directed NMR study on ^{13}C-labeled membrane proteins can serve as a convenient probe to reveal their local conformation and dynamics. We attempted here to clarify the extent to which ^{13}C NMR spectra of ^{13}C-labeled *fully hydrated* bacteriorhodopsin (bR) as a typical membrane protein are visible or well resolved in the presence of inherent fluctuation motions with frequency of 10^2–10^8 Hz, especially at the membrane surfaces. Accordingly, we estimated the relative proportion of ^{13}C NMR signals from the surface areas with and without peak suppression by the accelerated transverse relaxation effect by surface-bound Mn^{2+} ions, which could be effective for residues within 8.7 Å of the membrane surface. It turned out that the experimental findings are consistent with the predicted amount of amino acid residues under consideration located within 8.7 Å of the surface for [1-^{13}C]Val- and Ile-labeled bR and also [3-^{13}C]Ala-bR. In contrast, ^{13}C NMR peaks from such surfaces area are almost completely or partially suppressed for [1-^{13}C]Gly-, Ala-, Leu-, Phe- and Trp-labeled bR, as a result of plausible interference of the fluctuation frequency with frequency of magic angle spinning (10^4 Hz). We further assigned several ^{13}C NMR signals of [1-^{13}C] Val-, Trp- and Ile-labeled bR on the basis of a variety of site-directed mutants with reference to those of the wild type. Further, we recorded the ^{13}C NMR of bR in lipid bilayers to search for the optimal conditions to be able to obtain signals with the highest peak intensities and spectral resolution. Backbone dynamics turn out to be essential for recording ^{13}C NMR spectra so as to escape from motional frequencies of the order of 10^4–10^5 Hz, either in the direction of accelerated fluctuation or slowed motions in the direction of forming the 2D array.

KEYWORDS: NMR; site-directed ^{13}C NMR; membrane proteins: bacteriorhodopsin; cross-polarization magic angle spinning; dipolar decoupled magic angle spinning; dynamics; Mn^{2+}-induced transverse relaxation

INTRODUCTION

It is well recognized that membrane proteins play crucial roles in maintaining various activities of cells such as the transport of appropriate molecules into or out of the cell, catalysis of chemical reactions and receiving and transducing chemical signals from the cell environment.[1] Even though x-ray crystallography and multi-dimensional solution NMR spectroscopy have proved to be the most favorable standard approaches to determine the three-dimensional structure for a variety of biological molecules such as globular proteins, application of these approaches to a variety of membrane proteins is not always straightforward because of underlying problems such as extreme difficulty in crystallization and enormously broadened linewidths due to increased effective molecular mass caused by the possibility of oligomerization of constituent proteins and the presence of surrounding lipid molecules, respectively.

This is the reason why a high-resolution ^{13}C solid-state NMR approach is sought as an alternative means to this end in view of the large dispersion of chemical shifts, because their spectral resolution is no longer determined by the prolonged correlation times arising from the increased effective molecular mass but is mainly dependent on

*Correspondence to: Hazime Saitô, Department of Life Science, Graduate School of Science, Himeji Institute of Technology, Harima Science Garden City, Kamigori, Hyogo 678-1297, Japan.
E-mail: saito@sci.himeji-tech.ac.jp
Contract/grant sponsor: Ministry of Education, Science, Culture and Sports.

conformational homogeneity as in the crystalline state. Nevertheless, it should be anticipated that the spectral resolution of observed ^{13}C NMR signals to individual carbons will not always be straightforward for intact membrane proteins in view of heavily overlapped signals from the contribution of large amounts of amino acid residues involved. In addition, it should be taken into account that the ^{13}C NMR signals of fully ^{13}C-labeled proteins, such as [1,2,3-^{13}C]Ala-labeled bacteriorhodopsin (bR), were substantially broadened owing to the accelerated transverse relaxation rate coupled with inherent fluctuation motions of membrane proteins promoted by increased numbers of relaxation pathways through ^{13}C–^{13}C dipolar interactions and scalar couplings.[2] Accordingly, it is anticipated that the application of the recently developed multi-dimensional ^{13}C solid-state NMR[3,4] approach will not always be an effective remedy to overcome this problem as far as intact whole membrane proteins integrated in lipid bilayer are concerned.

As an alternative, we have developed a site-directed ^{13}C NMR approach[5,6] suitable for revealing the local conformation and dynamics of ^{13}C-labeled membrane proteins prepared from a single ^{13}C-labeled amino acid as a source of ^{13}C labeling instead of uniformly labeled preparations: the ^{13}C NMR signals of [3-^{13}C]Ala and [1-^{13}C]Val-labeled proteins were recorded by both cross-polarization magic angle spinning (CP/MAS) and *single pulse* dipolar decoupled magic angle spinning (DD/MAS) NMR techniques, with the expectation that ^{13}C NMR signals from more flexible residues located at the membrane surface can be readily distinguished from those of the transmembrane α-helices in view of their differential spin–lattice relaxation times. The resulting ^{13}C NMR signals were well resolved to yield 12 and 9 signals for [3-^{13}C]Ala- and [1-^{13}C]Val-bR of fully hydrated preparations, respectively, at ambient temperature, and consequently many such resolved peaks were assigned initially in a regiospecific manner based on the conformation-dependent displacements of ^{13}C NMR signals,[7–9] and subsequently in a site-directed manner in view of reduced peak intensities of site-directed mutants with reference to the peak of the wild type. In such a case, the ^{13}C NMR signals are almost fully visible[10] as far as [3-^{13}C]Ala-bR from a purple membrane consisting of 2D crystals of hexagonally packed trimeric forms[11] is concerned. In this way, we accomplished the assignment of the ^{13}C NMR signals (over 60%) from [3-^{13}C]Ala-bR and obtained much invaluable information about the conformation and dynamics of bR of biological significance under physiological conditions,[2,12–25] as summarized in Table 1.

In contrast, we found that the ^{13}C NMR signals of [1-^{13}C]- or [2-^{13}C]Ala-labeled interhelical loops and transmembrane α-helices of bR near the membrane surface are almost completely suppressed.[2] One of the reasons for this is that high-resolution ^{13}C NMR signals from such regions could be suppressed by the acquisition of fluctuation motions with frequency of the order of 10^4 Hz, which results in the failure of the high-resolution NMR process on magic angle spinning at 4 kHz owing to interference with coherent frequency of either proton decoupling or magic angle spinning.[26,27] This frequency, however, is indifferent to observation of the

Table 1. Conformation and dynamics of bacteriorhodopsin in relation to biological function revealed by site-directed ^{13}C NMR

	Ref.
Identification of C-terminal α-helix protruding from the membrane surface	2, 12, 13
Hydration- and temperature-dependent surface dynamics	14–16
Significance of cytoplasmic surface complex	16, 17
Location of cation binding site(s) and cation-induced structural changes	16, 18, 19
Backbone dynamics	2, 16
Long-distance interactions among residues along the proton transfer pathways	20–22
Dynamics of M-like state	23
Significance of lipid–protein and protein–protein interactions in relation to formation of a 2D array	24
Conformation and dynamics changes of phoborhodopsin (sensory rhodopsin II) complexed with cognate transducer	25

^{13}C NMR spectra of [3-^{13}C]Ala-bR mentioned above, which could be suppressed in the presence of fluctuation motions with frequency 10^5 Hz interfered with the proton-decoupling frequency.[28] This is the reason why [3-^{13}C]Ala-bR in a purple membrane is the most favorable system as far as ^{13}C NMR measurements are concerned. Nevertheless, we found that several ^{13}C NMR signals are readily visible from loops when the ^{13}C NMR spectra of [1-^{13}C]Val-bR were examined.[20,21] This means that the manner of peak suppression may also be dependent on the type of labeled amino acid residues as intrinsic probes. To clarify this problem, it is very important to gain insight into the critical conditions to cause suppression of the ^{13}C NMR signals from such interhelical loops for a variety of [1-^{13}C]amino acid-labeled bR. For this purpose, we compared the ^{13}C NMR peak intensities between intact and Mn^{2+}-treated preparations, because it is expected that ^{13}C NMR signals under consideration might be consistent with those preferentially broadened by accelerated spin relaxations by surface-bound Mn^{2+} ions as relaxation agent.[29,30] This approach permits one also to identify single carbon signals from heavily overlapped signals, if the contribution from partially suppressed ^{13}C NMR signals, if any, mainly from residues located at the surface, is readily removed by Mn^{2+}-induced peak suppression.

In this work, we compared the ^{13}C NMR spectra of bR labeled with [1-^{13}C]Gly, -Val, -Trp, -Phe, -Leu and -Ile with and without surface-bound Mn^{2+} ions, to shed light on the above-mentioned problems. The relative proportion of carbon signals was counted by deconvolution of the observed spectra with reference to the peak intensity of identified single carbon from the inner part of the transmembrane α-helix which is indifferent to a plausible peak suppression by spin relaxation by the surface-bound Mn^{2+} ions. We have also recorded ^{13}C NMR spectra of a variety of [1-^{13}C]Val-labeled site-directed mutants in order to assign peaks of Val29, -34,

-130, -136, -151, -167, -179, -187, -217, etc., and some Trp and Ile mutants, based on comparative examination of the ^{13}C NMR spectra between wild-type and appropriate mutants. Finally, we compared the ^{13}C NMR spectra of [3-^{13}C]Ala-bR integrated in egg PC bilayers at various temperature with that of the purple membrane, in order to search for the optimal conditions to be able to record ^{13}C NMR signals of membrane proteins with improved sensitivity and well-resolved signals.

EXPERIMENTAL

[1-^{13}C]Gly, -Leu, -Val, -Trp and -Ile were purchased from CIL (Andover, MA, USA) and used without purification. A variety of mutants, V29A, V34A, V130A, V136A, V151A, V179M, V180A, V187L, V213A, V217A, W182F and W189F (see Fig. 1 for their locations), were constructed as described by Needleman *et al*.[31] *H. salinarum* S9 and the above-mentioned mutants were grown in the TS medium of Onishi *et al*.[32] in which unlabeled amino acid residues under consideration were replaced by one of the above-mentioned isotopically labeled amino acid residues. Bacteriorhodopsin (bR) was isolated and purified as a purple membrane by the method of Oesterhelt and Stoeckenius[33] and subsequently resuspended in 5 mM HEPES buffer (pH 7.0) containing 10 mM NaCl and 0.025% NaN_3. Some of these preparations were treated by resuspension in the presence of 40 μM $MnCl_2$ in the above-mentioned buffer to adjust the final optical density of the chromophore to 1.00. The membrane preparations were finally concentrated by centrifugation and placed in a 5 mm o.d. zirconia pencil-type sample rotor for magic sample spinning and the caps were tightly sealed with glue to prevent evaporation of water.

Site-directed solid-state ^{13}C NMR spectra were recorded in the dark at ambient temperature on a Chemagnetic CMX-400 Infinity NMR spectrometer by CP/MAS and DD/MAS methods. The spectral width, acquisition time and repetition time for the CP/MAS experiment were 40 kHz, 50 ms and 4 s, respectively. The 90° pulse for carbon and proton was 5.0 μs and the spinning rate was 4 kHz. The contact time for the CP/MAS experiment was 1 ms. Free induction decays were acquired with 2K data points and Fourier transformed as 16K data points after 14K data points had been zero-filled. The 45° pulse and a repetition time of 6 s were used to record ^{13}C NMR spectra by the DD/MAS NMR method. The ^{13}C chemical shifts were initially referred to the carboxyl signal of crystalline glycine [176.03 ppm from tetramethylsilane (TMS)] and then expressed as relative shifts from TMS. Spectral deconvolution was performed either by a software package provided by Chemagnetics or PeakFit for Windows, to estimate the carbon numbers involved in a single peak.

THEORETICAL BACKGROUND FOR IDENTIFICATION OF ^{13}C NMR SIGNALS FROM RESIDUES LOCATED NEAR THE SURFACE

The ^{13}C NMR signals of residues located at the loop and transmembrane α-helices near the surface could be preferentially broadened by dipole–dipole interaction between Mn^{2+} ion and the ^{13}C atom under consideration. This interaction is expressed as a function of distances between electron and nuclear spin (r) and the correlation time of rotational reorientation of the spin pair (τ_r), according to the Solomon–Bloembergen equation:[29,30]

$$1/T_{2c} = [S(S+1)\gamma_c^2 g^2 \beta^2]/15r^6][(4\tau_{c_1} + 3\tau_{c_1})/(1+\omega_c^2\tau^2_{c_1}) + 13\tau_{c_2}/(1+\omega_e^2\tau^2_{c_2})] \quad (1)$$

$$1/\tau_{c_1} = 1/T_{1e} + 1/\tau_r + 1/\tau_m; \qquad 1/\tau_{c_2} = 1/T_{2e} + 1/\tau_r + 1/\tau_m$$

where T_{2c} is the spin–spin relaxation time of a ^{13}C nucleus, r is the distance between the ^{13}C nucleus and Mn^{2+} ion, S is the total electron spin, ω_c and ω_e are the nuclear and electronic Larmor precession frequencies, respectively, γ_c is the gyromagnetic ratio of ^{13}C, g is the g-factor of Mn^{2+}, β is the Bohr magneton, T_{1e} and T_{2e} are the spin–lattice and spin–spin relaxation times of an electron, respectively, τ_r is the rotational correlation time of the Mn^{2+}–bR complex and τ_m is the lifetime of the Mn^{2+} complex. The g-factor and T_{1e} of Mn^{2+} are assumed to be identical with those of an aqua ion. τ_m is assumed to be longer than $T_{1e}(3 \times 10^{-9}$ s). When τ_r is longer than T_{1e}, it is expected that the linewidth corresponding to the calculated T_{2c} value becomes greater than 100 Hz in the area within 8.7 Å from the Mn^{2+} ion at negatively charged amino acid residues, as illustrated by the shaded area in Fig. 1.[19] It turned out that a prediction based on this diagram is consistent with recent experimental data utilizing 40 μM Mn^{2+} ion to select the three ^{13}C NMR peaks from 1-^{13}C-labeled Pro residues located in the inner part of the transmembrane α-helices, Pro-50, -91 and -186.[34]

In spite of currently available *static* picture of bR obtained by diffraction data for either 2D or 3D crystals at cryo-temperatures, we showed that fully hydrated bR from the purple membrane at ambient temperature undergoes fluctuation motions with frequencies from 10^8 to 10^2 Hz, depending on its location.[2,22,24] This means that the resulting ^{13}C NMR linewidths ($1/\pi T_2^C$) from such regions could be substantially broadened as a result of failure of attempted peak narrowing, when the frequency of incoherent random fluctuations in such an area of the order of 10^4–10^5 Hz is interfered with by either the frequency of the magic angle spinning or proton decoupling.[26,27] It is expected that this happens when the second or third terms of Eqn (2) are made dominant over the first term $(1/\pi T_2^C)^S$ of the static component:[26,27]

$$1/\pi T_2^C = (1/\pi T_2^C)^S + (1/\pi T_2^C)^M{}_{DD} + (1/\pi T_2^C)^M{}_{CS} \quad (2)$$

where $(1/T_2^C)^M{}_{DD}$ and $(1/T_2^C)^M{}_{CS}$ are the transverse components due to the fluctuations of dipolar and chemical shift interactions, respectively. The last two terms are given as a function of the correlation time τ_c by

$$(1/T_2^C)^M{}_{DD} = \Sigma(4\gamma_I^2\gamma_S^2 h^2/15r^6)I(I+1)[\tau_c/(1+\omega_I^2\tau_c^2)] \quad (3)$$

$$(1/T_2^C)^M{}_{CS} = (\omega_0^2\delta^2\eta^2/45)[\tau_c/(1+4\omega_r^2\tau_c^2) + 2\tau_c/(1+\omega_r^2\tau_c^2)] \quad (4)$$

where γ_I and γ_S are the gyromagnetic ratios of I and S nuclei, respectively, and r is the internuclear distance between spins I and S; ω_0 and ω_I are the carbon resonance frequency and the

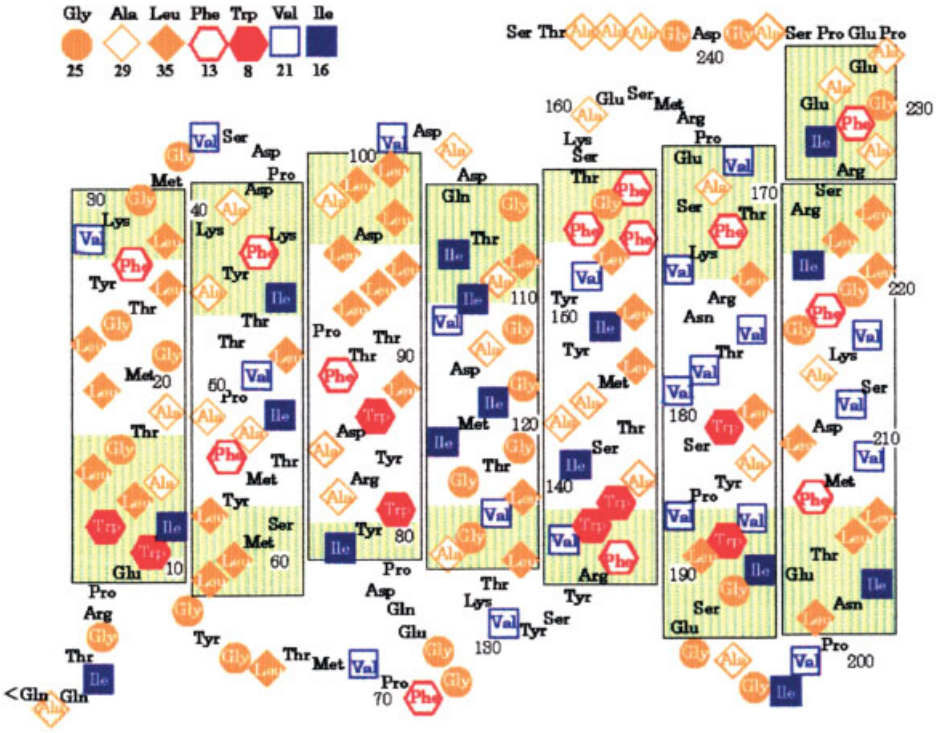

Figure 1. Schematic representation of secondary structure of bR based on x-ray diffraction studies. Residues within 8.7 Å of the negatively charged residues are shaded green color.[19] The numbers of included respective amino acid residues are shown below the symbols.

amplitude of the proton decoupling r.f. field, respectively; ω_r is the rate of spinner rotation; δ is the chemical shift anisotropy and η is the asymmetric parameter of the chemical shift tensor. As pointed out previously,[2,5,6] the contribution of the third $(1/T_2^C)^M{}_{CS}$ term of Eqn (2) is dominant when the fluctuation frequency of carbonyl or C_α carbons with larger chemical shift anisotropy is close to the extent of magic angle spinning, 4 kHz (ω_r). In fact, we showed that ^{13}C NMR signals from the surface areas were completely suppressed as viewed from the ^{13}C NMR peaks of [1-^{13}C]- and [2-^{13}C]Ala-bR.[2] We also demonstrated that the observation of such selectively suppressed ^{13}C NMR peaks due to interference of motional frequency with frequency of either proton decoupling or magic angle spinning can be conveniently utilized as intrinsic probes for backbone dynamics in relation to biological functions, as summarized in Table 1.

RESULTS AND DISCUSSION

Evaluation of the ^{13}C NMR signals from membrane surface based on Mn^{2+}-induced suppressed peaks

We recorded the ^{13}C NMR spectra of bR labeled with [1-^{13}C]Gly, -Leu, -Trp, -Phe, -Val and -Ile in the presence (dotted traces) or absence (solid traces) of 40 μM Mn^{2+} ion as illustrated in Figs 2–6, to evaluate the contribution of ^{13}C NMR signals from membrane surface. It appears from Fig. 2 that a broad envelope centered at 175 ppm is present as a background signal in addition to the main peak of [1-^{13}C]Gly-labeled bR which is ascribed to several superimposed ^{13}C NMR signals from amino acid residues with substituents at C_α[7–9] of natural abundance nuclei such as Ala, Leu and Val [Fig. 2(A) and (B)]. Instead, the intense ^{13}C NMR peak at 171.7 ppm from the CP/MAS and DD/MAS NMR spectra arose from the α-helical segments as viewed from the conformation-dependent ^{13}C chemical shifts for [1-^{13}C]Gly residues.[7,8] In general, the ^{13}C CP/MAS NMR signals of bR labeled with [1-^{13}C]amino acid residues, except for Gly, spread over the region between 171 and 178 ppm. In particular, the ^{13}C signals resonating at lower field than 174.9 ppm are ascribed to those of the α-helix, whereas the higher field signals than this are assigned to either a turned structure or β-sheet.[5–9] The intense ^{13}C NMR signal of [1-^{13}C]Leu-bR as recorded by DD/MAS NMR [Fig. 2(C)], however, is undoubtedly ascribed to a scrambled peak from incorporated [1-^{13}C]Leu, because no such signal is present in the corresponding CP/MAS NMR spectrum [Fig. 2(D)].

In Figs 3(B) and 4(D), we illustrate the ^{13}C DD/MAS NMR spectra of [1-^{13}C]Phe- and -Trp-bR, respectively. Surprisingly, the relative intensities of these peaks obtained by DD/MAS NMR are almost the same as those recorded by the CP/MAS experiment, except for the presence of several asterisked peaks in the latter, probably arising from signals due to a scrambled isotope. In general, it is well recognized that recording ^{13}C NMR signals by means of the DD/MAS method from the transmembrane α-helices of bR labeled with [1-^{13}C]amino acids is very difficult in view of their generally longer spin–lattice relaxation times, of the order of 10–20 s.[2] Surprisingly, we noted that such signals were observed by the DD/MAS method, probably because the ^{13}C spin–lattice relaxation times from the transmembrane α-helices of [1-^{13}C]Phe- and -Trp-bR are shortened by at least one order of magnitude compared with those of other amino

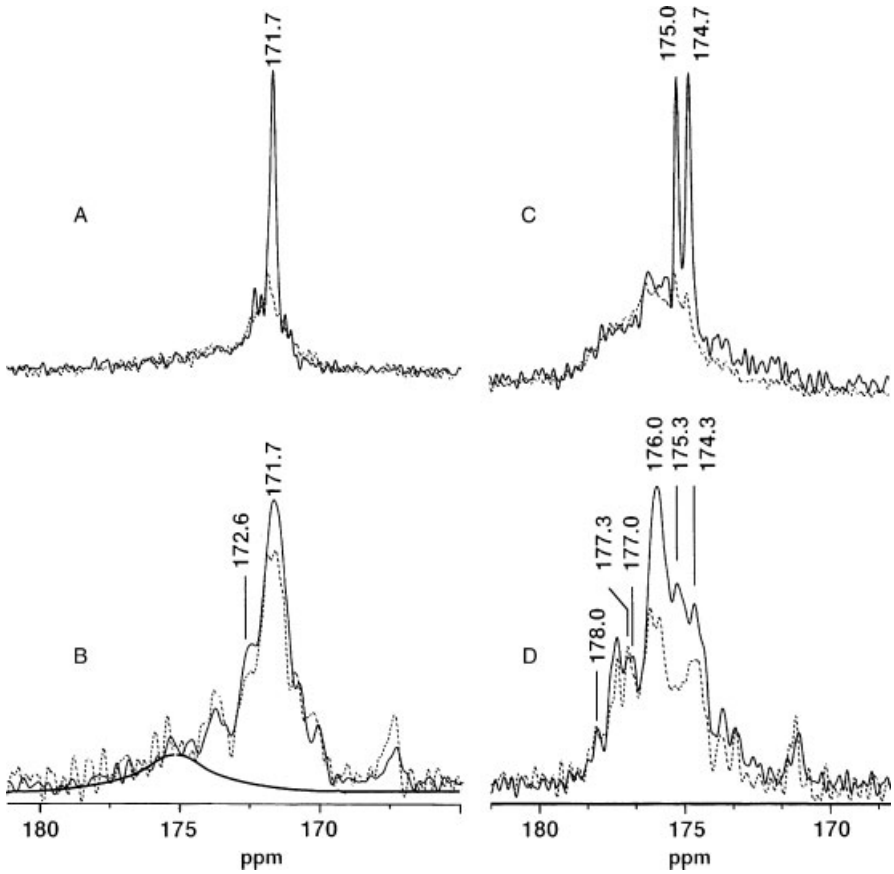

Figure 2. ^{13}C DD/MAS (A and C) and CP/MAS (B and D) NMR spectra of [1-^{13}C]Gly- and -Leu-labeled bR, respectively, without (solid traces) and with 40 μM Mn^{2+} ion (dotted traces).

acid residues such as Gly, Ala and Val.[2] It appears that this is caused by the presence of the two-site jump motions of these aromatic side-chains especially in the membrane environment which could serve as a sink for the shortened spin–lattice relaxation times.[35,36]

It is noteworthy that the ^{13}C NMR signals of [1-^{13}C]Val- and -Ile-bR were substantially suppressed in the presence of 40 μM Mn^{2+} ion, in view of the transverse spin relaxation rate from surface-bound Mn^{2+} ion[18,19] [see Eqn (1)],[19] as demonstrated in Figs 5 and 6. In such cases, the relative contributions of the ^{13}C NMR signals from the surface areas as estimated as $1 - I/I_0$, by comparison of the peak intensities with (I) and without (I_0) Mn^{2+} ion, are in good agreement with the amounts of the respective residues estimated from the expected number of these residues within 8.7 Å of the negatively charged residues,[19] as summarized in Table 2. In contrast, we found that the relative contributions of the ^{13}C NMR signals from the surface areas are substantially lower than the expected values: they are 0.12, 0 and 0.11 for [1-^{13}C]Gly-, -Ala-[24] and -Leu- bR, respectively, while the expected data based on predicted number of these residues from the surface areas are 0.67, 0.62 and 0.49, respectively (see Table 2). These findings indicate that ^{13}C NMR signals from the surface areas of these systems are substantially suppressed even in the absence of Mn^{2+} ion, caused by interference of incoherent low-frequency fluctuation motions with the coherent frequency of magic angle spinning, as demonstrated for [1-^{13}C]Ala-bR.[24,37] This is true for the ^{13}C

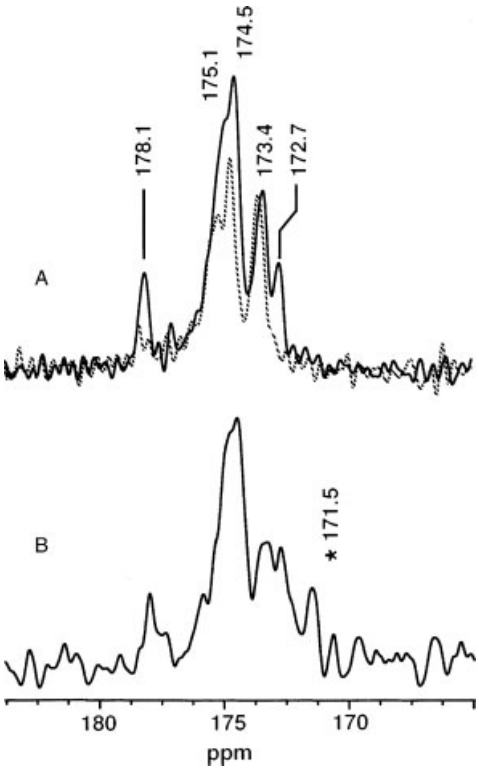

Figure 3. ^{13}C CP/MAS (A) and DD/MAS (B) NMR spectra of [1-^{13}C]Phe-labeled bR. The dotted trace (A) was obtained in the presence of 40 μM Mn^{2+} ion. The asterisked peak is visible only by the latter method.

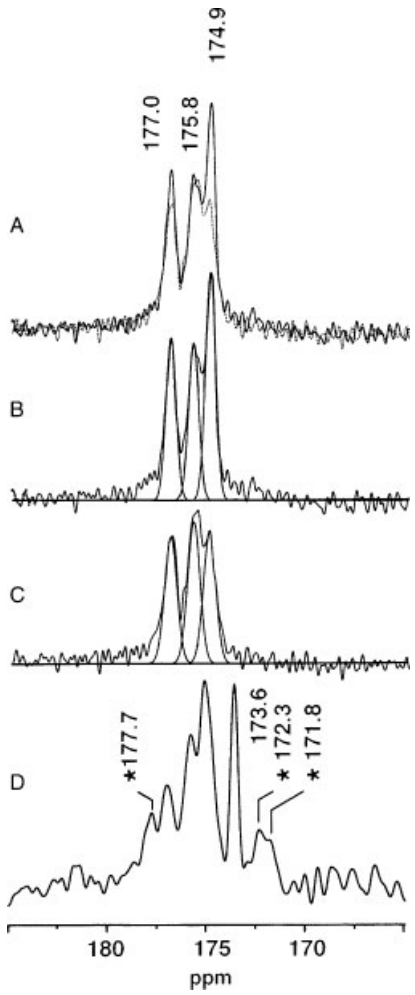

Figure 4. ^{13}C CP/MAS NMR spectra of [1-^{13}C]Trp-labeled bR without (solid trace) and with 40 μM Mn^{2+} ion (dotted trace) (A), deconvoluted spectra without (B) and with 40 μM Mn^{2+} ion (C), and corresponding ^{13}C DD/MAS NMR spectrum (D). Several asterisked peaks arose from ^{13}C signals probably scrambled from incorporated [1-^{13}C]Trp.

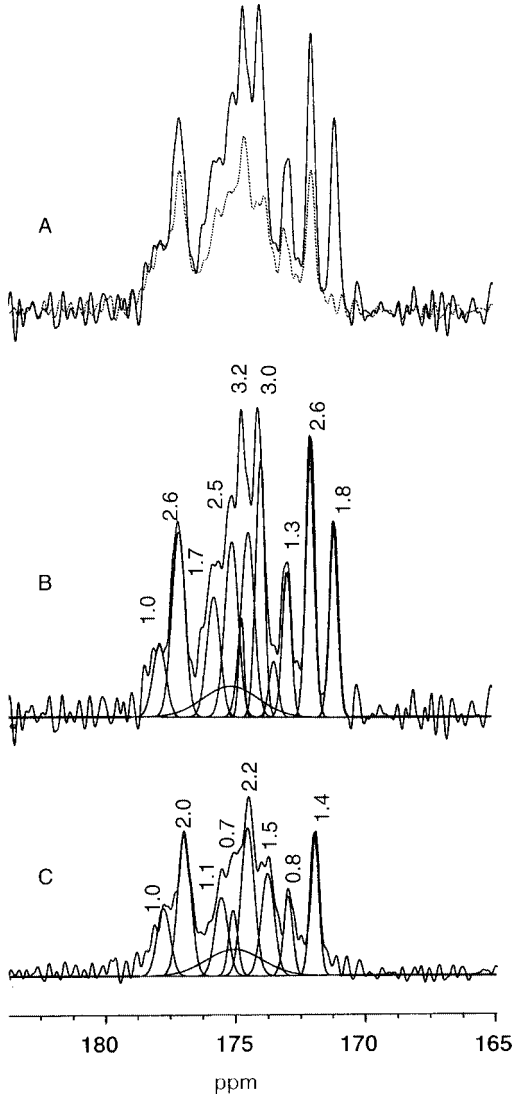

Figure 5. ^{13}C CP/MAS NMR spectra of [1-^{13}C]Val-labeled bR without (solid traces) and with 40 μM Mn^{2+} ion (dotted trace) (A), deconvoluted spectra without (B) and with 40 μM Mn^{2+} ion (C).

NMR peak intensities of [1-^{13}C]Phe- and -Trp-bR: they are lower than the predicted relative amounts of these residues from the membrane surface (see Table 2).

It appears, therefore, that the presence of such low-frequency, *residue-specific dynamics*, leading to completely or partially suppressed peaks in the absence of Mn^{2+} ion, is well related to the possibility of conformational fluctuations caused by the time-dependent deviation from the torsion angles corresponding to the lowest energy minimum of particular conformation. Naturally, it is conceivable that such conformational space allowed for fluctuation motion may be limited to a very narrow area for Val or Ile residues with bulky side-chains at C_α, together with limited χ_1 rotation around the C_α—C_β bond as shown by C_α—$C_\beta H(X)(Y)$ where X and Y are substituents on C_β. In contrast, this minimum may be very shallow for Gly residues in view of the widely allowed conformational space. In this connection, it is plausible that the above-mentioned low-frequency, residue-specific backbone dynamics are present for Ala, Leu, Phe and Trp residues, because backbone dynamics in these systems could be coupled with a possible rotational motion of the χ_1 angle around the C_α—C_β bond, as represented schematically by the C_α—$C_\beta H_2$—Z system, where Z is H, isopropyl, phenyl or indole.

Deconvoluted peaks

It is also very useful to estimate the relative proportions of carbons contributing to individual peaks by means of deconvoluted spectra without and with Mn^{2+} ion as indicated in the lower part of Figs 4–6. The ^{13}C NMR peak intensities of the carbonyl signals turned out to be not always integers but decimal, as illustrated by values above the individual peaks in italics, in contrast to our previous ^{13}C NMR data on [3-^{13}C]Ala-bR, because these ^{13}C NMR signals could be partially suppressed by interference of fluctuation frequency with the frequency of magic angle spinning, as demonstrated in Eqns (2) and (3). As illustrated in Fig. 4, only three peaks were resolved for the ^{13}C NMR spectra of [1-^{13}C]Trp-bR. These numbers are readily evaluated by simple inspection of the secondary structure illustrated in

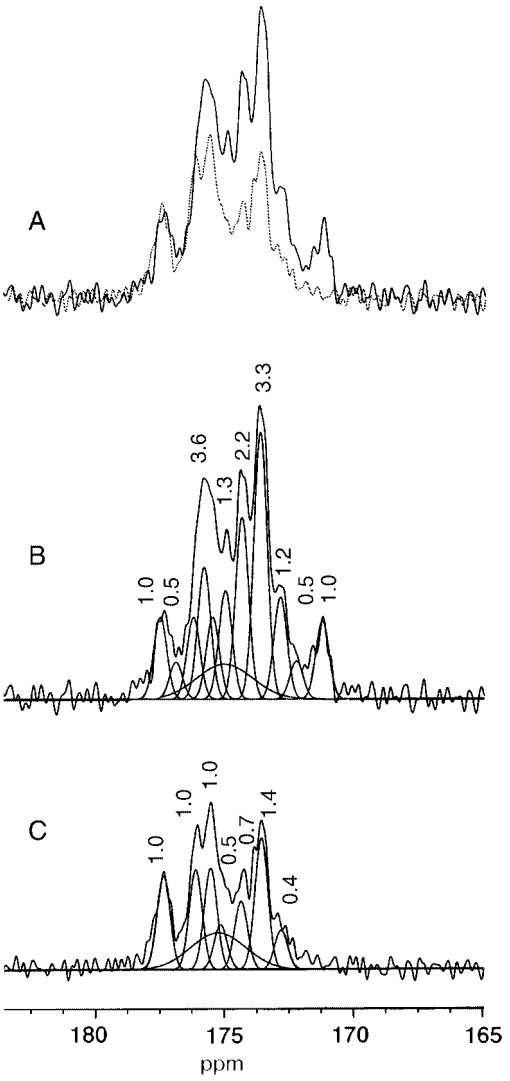

Figure 6. ^{13}C CP/MAS NMR spectra of [1-^{13}C]Ile-labeled bR without (solid traces) and with 40 μM Mn^{2+} ion (dotted trace) (A), deconvoluted spectra without (B) and with 40 μM Mn^{2+} ion (C).

Fig. 1: two Trp residues are located in the green-coloured shaded area among the total eight Trp residues. To estimate the deconvoluted ^{13}C NMR signals for [1-^{13}C]Val- and -Ile-bR, the contribution from the broad envelope from signals of natural abundant nuclei [Fig. 2(B)] was subtracted. The estimated numbers of carbons for intact and Mn^{2+}-treated spectra for Val residues are thus 23 and 13, respectively, if one counts decimals as one (Fig. 5). The numbers of residues are 21 and 11–13, respectively. In addition, there are 16 Ile residues in total and seven Ile residue within the areas of membrane surfaces indicated by shading. Consistent with this, the total peak intensities for Ile residues based on deconvolution of the intact and Mn^{2+}-treated preparations for the individual peaks are 17 and 8, respectively (Fig. 6).

Site-directed assignment of ^{13}C NMR signals: [1-^{13}C]Val-bR

The above-mentioned manner of counting the contributed numbers of carbon nuclei is obviously far from quantitative. Therefore, the most reliable means is to count the individual peaks of assigned ones based on comparison of the peak intensities between the wild-type and respective site-directed mutant. As demonstrated in Fig. 7, the ^{13}C CP/MAS NMR spectra of [1-^{13}C]Val-labeled V213A, V29A, and V34A were compared with those of the wild type (top trace), to give rise to assigned peaks indicated in the top trace from the data presented here and also the data to be described below. Obviously, both Val-29 and V213 were ascribed to the intense low-field peak at 177.04 ppm (ca 2.6 carbons), because the peak intensities of these peaks were reduced for V213A and V29A mutants. Minor peak changes at 173.97 and 174.60 ppm, however, were also present owing to local dynamics changes in the transmembrane α-helices in these mutants. In a similar manner, Val-217 was ascribed to the peak at 174.97 ppm (ca 1.6 carbons) with reference to the data for the V217A mutant, whereas Val-136, -179 and -187 were ascribed to the peak at 174.60 ppm (3 carbons) in view of the reduced peak intensities in the ^{13}C CP/MAS NMR spectra of V136A, V179M and V187L with reference to the data for the wild type (Fig. 8). The assignment of peaks to Val-130, -151 and -180, however, turned out not always to be straightforward: in such cases, the two peaks for both transmembrane α-helix and loop were changed simultaneously as shown by the ^{13}C NMR peaks of the corresponding mutants as indicated by the wedges in Fig. 9. In particular, it turned out that the site-directed mutation at Val-130 in the D–E loop resulted also in spectral changes in the transmembrane α-helix, while mutation at Val-180 in helix F resulted in spectral changes in the loop region. Here, we adopted the assignment of peaks at 171.99 and 173.97 ppm to Val-130 and -180, respectively, by taking into account of the range of the conformation-dependent displacement of peaks so far accumulated and also their locations in the secondary structure as deduced by x-ray diffraction studies. Surprisingly, it is noted that Val-151 located at helix F is in a state to be able to undergo flexible motions as judged from the reduced spin–lattice relaxation times which enable one to observe the ^{13}C NMR signals in the DD/MAS NMR spectra. This kind of conformational

Table 2. Comparison of relative proportion of the ^{13}C NMR signals from the surface areas as estimated from the ^{13}C NMR intensity ratio with (I) and without (I_0)Mn^{2+} ion

	Estimated from ^{13}C signals $(1 - I/I_0)$	Predicted amounts of residues near the surface (8.7Å from the membrane surface)	Suppressed ^{13}C NMR peaks from the surface area caused by slow motions
Gly	0.14	0.67	Suppressed
Ala	~0[a]	0.62	Almost completely suppressed
Leu	0.11	0.49	Suppressed
Phe	0.24	0.55	Suppressed
Trp	0.24	0.38	Suppressed
Val	0.41	0.38	None
Ile	0.50	0.56	None

[a] Ref. 24.

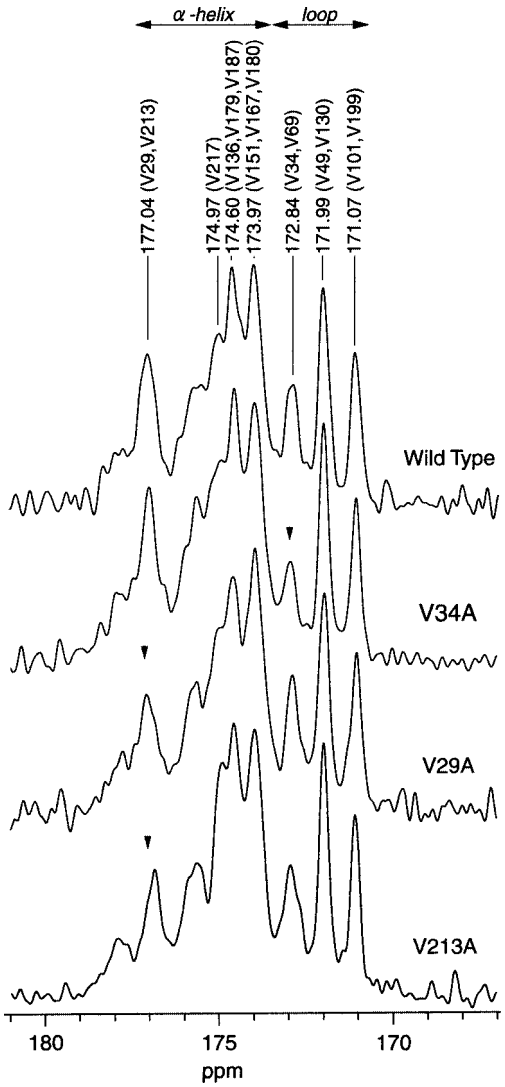

Figure 7. ^{13}C CP/MAS NMR spectra of [1-^{13}C]Val-labeled wild-type, V29A, V34A and V213A mutants. Peaks with reduced intensities due to the site-directed mutation corresponding to the site for mutation are indicated by wedges.

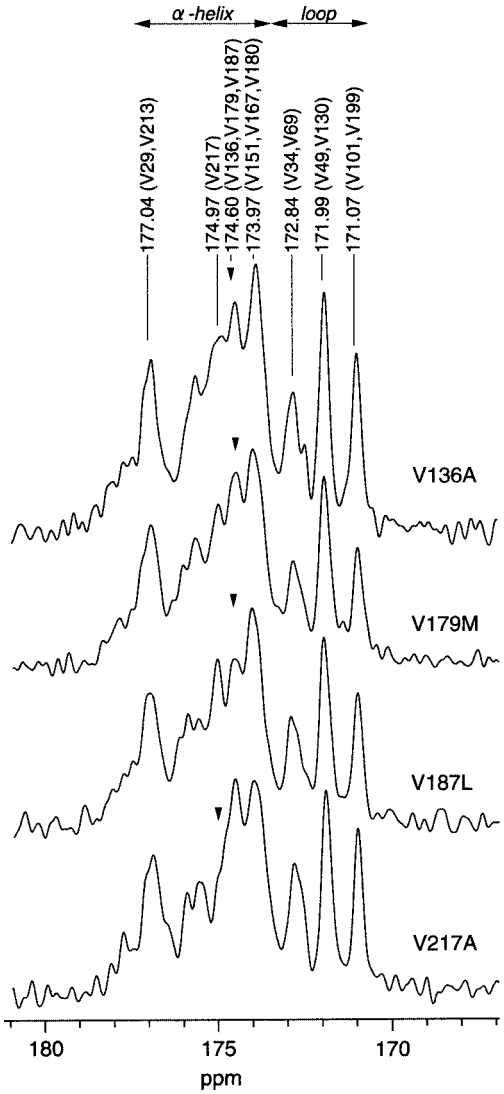

Figure 8. ^{13}C CP/MAS NMR spectra of [1-^{13}C]Val-labeled V136A, V179M, V187L and V217A mutants. Peaks with reduced intensities due to the site-directed mutation corresponding to the site for mutation are indicated by wedges.

flexibility seems to be essential for efficient backbone motions during photocycles.

As illustrated in Fig. 9, the ^{13}C NMR peak position resonating at 177.04 ppm seems to be well related with the variation of the UV absorption maximum of bR including blue membrane,[17] R82Q[21] and D85N[22] mutants, and can be utilized as a convenient probe around the Schiff base. This is because the peak for Val-213, resonating at such low field, could be characterized as a residue with a very short hydrogen bond length together with that of the bifurcated hydrogen bond network, and could be utilized as a probe for the environment around the Schiff base (to be discussed later).

Site-directed assignment of peaks: [1-^{13}C]Trp and Ile

In order to assign the ^{13}C NMR peaks to Trp-182 and -189 residues, we compared the ^{13}C CP/MAS NMR spectra of W189F [Fig. 10(A)] and W182F mutants [Fig. 10(B)] with those of the wild type as illustrated in Fig. 10. In view of the obviously reduced peak intensities in these mutants, the ^{13}C NMR signals resonating at 175.8 and 175.0 ppm were straightforwardly assigned to Trp-182 and -189, respectively. It was very difficult, however, to assign the ^{13}C chemical shifts of Trp-12 and -80 in this manner, because all the ^{13}C signals of W12L and W80L mutants were completely suppressed (spectra not shown). In addition, we recorded the ^{13}C DD/MAS NMR spectrum of the [1-^{13}C]Ile-labeled wild type [Fig. 11(A)] and the CP/MAS NMR spectra of [1-^{13}C]Ile-labeled I222C [Fig. 11(B)] and the wild type [Fig. 11(C)] for assignment of the peak for Ile-222. The obviously reduced ^{13}C NMR peak at 175.7 ppm in the I222C mutant was straightforwardly ascribed to Ile-222. The intense peak at 173.5 ppm in the DD/MAS spectrum is assigned to Ile-4 at the N-terminus taking a random coil conformation. The two signals resonating at higher field than the peak for random coil, 171.2 and 172.9 ppm, are assigned to Ile-78 and -198 of the B–C loop (see Fig. 1), respectively, or vice versa. Finally,

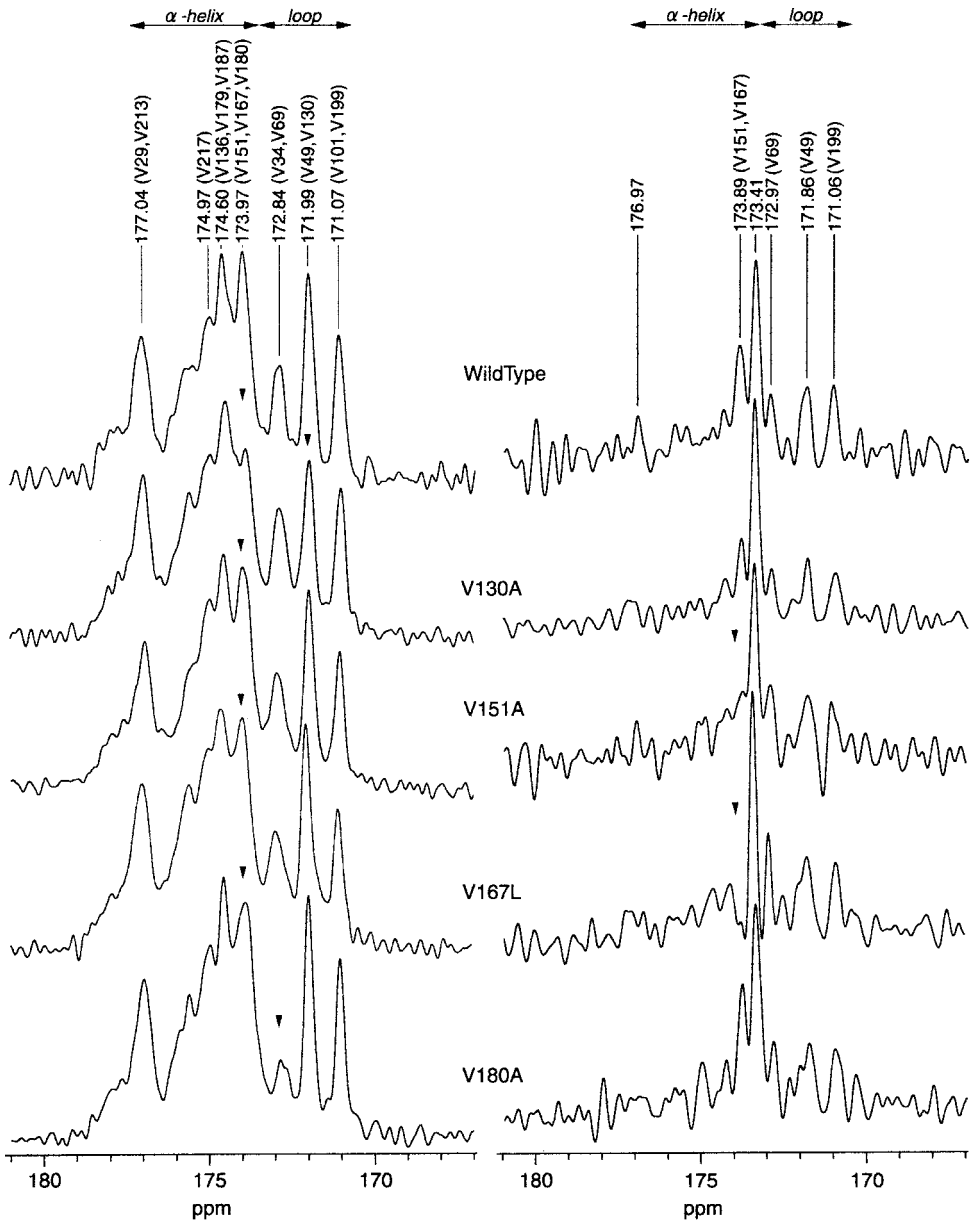

Figure 9. ^{13}C CP/MAS (left) and DD/MAS NMR (right) spectra of [1-^{13}C]Val-labeled wild-type, V130A, V151A and V180A mutants. Peaks with reduced intensities due to the site-directed mutation corresponding to the site for mutation are indicated by wedges.

the two intense signals in the ^{13}C DD/MAS spectrum of [1-^{13}C]Leu-bR resonating at 175.0 and 174.7 ppm [Fig. 2(C)] are straightforwardly ascribed to Leu-66 in spite of the presence of two peaks, because they are preferentially suppressed in the presence of Mn^{2+} ion and L66A mutant (data not shown).

Backbone dynamics for the optimum condition to record ^{13}C NMR spectra of ^{13}C-labeled membrane proteins

We have so far discussed the spectral features of the ^{13}C NMR spectra of ^{13}C-labeled bR from purple membrane taking 2D crystals in which the trimeric unit of bR is hexagonally packed.[11] It should be anticipated, however, that such oligomerization and also lattice formation are not always straightforward for a variety of membrane proteins overexpressed from a host cell such as *E. coli.* As a result, it seems essential to record the ^{13}C NMR signals of reconstituted membrane proteins in lipid bilayers which are most likely to be present in a monomeric form. It is therefore very important to clarify the extent to which the expected ^{13}C NMR spectra available from the 2D crystalline state are reproduced in lipid bilayers, because ^{13}C NMR spectral features are known to be strongly affected by backbone dynamics, which could be influenced by the manner of protein–protein and lipid–protein interactions.[38] In this connection, we have shown previously that the ^{13}C NMR signals of W80L and W12L mutants taking a disrupted or disorganized crystalline lattice, respectively, due to modified protein–protein and lipid–protein interactions essential for oligomerization,[35] exhibited a very broad ^{13}C NMR spectral envelope with reduced peak intensities for [3-^{13}C]Ala-bR and almost completely suppressed ^{13}C NMR signals for [1-^{13}C]Ala- or -Val-labeled preparations, respectively.[24] In contrast, we have recently shown that [3-^{13}C]Ala, [1-^{13}C]Val-labeled *pharaonis*

phoborhodopsin[25] (*p*pR, or sensory rhodopsin II) overexpressed in *E. coli* gave rise to well-resolved ^{13}C NMR signals, better than those of W80L and W12L mutants[24], although the ^{13}C NMR signals from the loops and some transmembrane α-helices are still missing. It is therefore very important to search for the optimal conditions to be able to record the full ^{13}C NMR spectra of bR integrated in lipid bilayers similar to those from purple membrane.

For this purpose, we compared the ^{13}C NMR spectra of [3-^{13}C]Ala-labeled W80L mutant (A) and bR in egg PC bilayer at ambient temperature (B) and at $-10\,^{\circ}C$ (C) as shown in Fig. 12. Interestingly, better spectral resolution was achieved for the ^{13}C NMR spectra of [3-^{13}C]Ala-bR in an egg PC bilayer than those of W80L mutant, in spite of the similarity of both preparations in the monomeric form [see the right parts in Fig. 12(A) and (B)]. It is emphasized that the spectral pattern of bR in egg PC obtained is very similar to that observed for *p*pR mentioned above.[25] In contrast, the ^{13}C NMR spectra of [1-^{13}C]Val-bR in an egg PC bilayer is much better than those of W80L in purple membrane, although the ^{13}C NMR signals from the loop region of [3-^{13}C]Ala-bR resonating at a peak position lower than 16.88 ppm were completely suppressed and signals from the cytoplasmic ends resonating 16.22–16.88 ppm are partially suppressed,[39] consistent with our previous findings about *p*pR in egg PC bilayers.[25] It is noteworthy, however, that such suppressed ^{13}C NMR signals were substantially recovered at $-10\,^{\circ}C$ to yield a spectral pattern similar to that in Fig. 13(C). This is probably caused by the possible participation of bR in a 2D array, although it is not always complete as

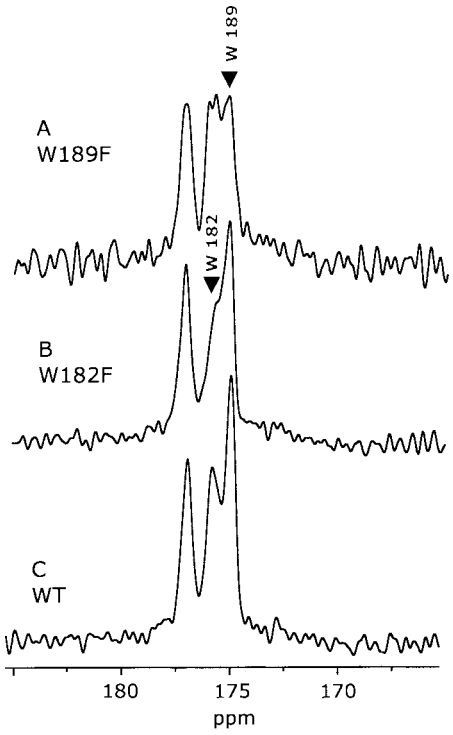

Figure 10. ^{13}C CP/MAS NMR spectra of [1-^{13}C]Trp-labeled W189F (A), W182F (B) and wild-type (C). The reduced peak intensities due to introduction of the mutation are indicated by wedges.

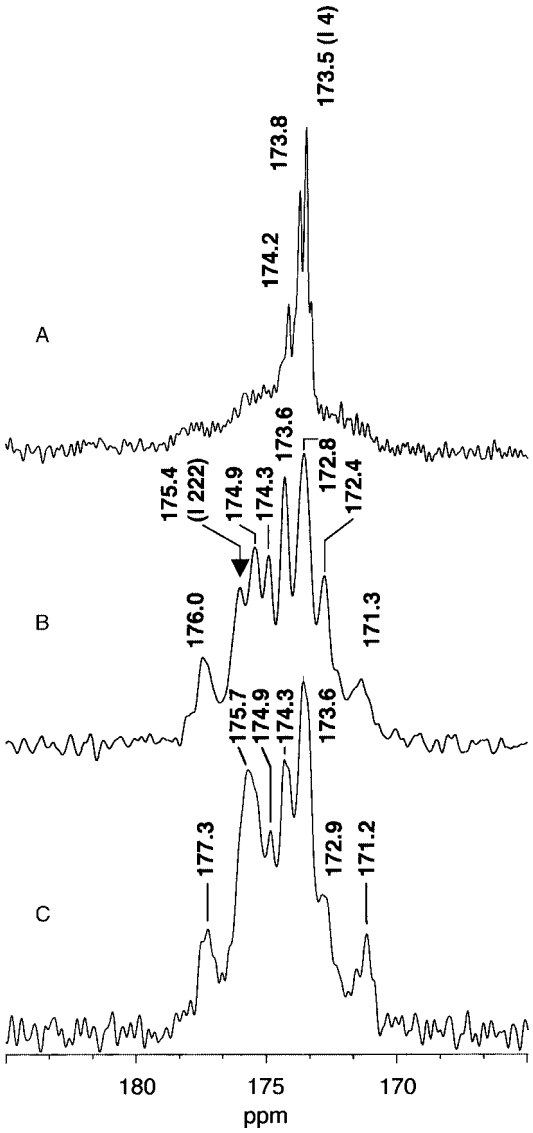

Figure 11. ^{13}C DD/MAS (A) and CP/MAS NMR spectra (B and C) of [1-^{13}C]Ile-labeled wild-type, I222C mutant and wild-type, respectively. The reduced peak intensity due to introduction of the mutation is indicated by a wedge.

a 2D lattice even at such low temperatures. Previously, Watts and co-workers demonstrated that 2D arrays could be formed in a reconstituted system in the presence of neutral and annular (or polar) lipids, at low temperatures below zero and at high ionic strength.[40–43] They showed that the latter lipids interact more strongly with the protein than the former. The present bR preparation isolated from purple membrane is obviously associated strongly with such polar lipids, as manifested by the presence of an intense peak at 19.8 ppm [see Fig. 12(B), right].[10,24] Therefore, the spectral pattern shown in Fig. 12(C) can be well recognized as a 2D array, although the ionic strength of the 10 mM NaCl used for this experiment is low as compared with the previous experiments.[40,41] In this connection, it has been demonstrated that the ^{13}C NMR spectral features of reconstituted bR were almost completely recovered in the gel-phase lipids of the DMPC or DPPC bilayer at $0\,^{\circ}C$.[39] This was also rationalized when the ^{13}C NMR spectra of [1-^{13}C]Val-bR [Fig. 12(C),

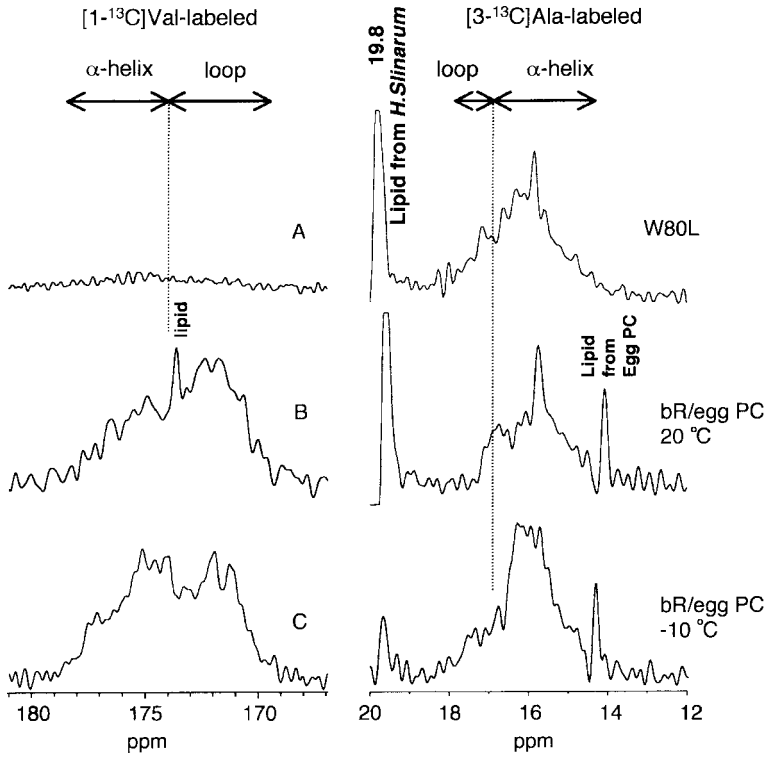

Figure 12. ^{13}C CP/MAS NMR spectra of [1-^{13}C]Val- (left) and [3-^{13}C]Ala-labeled W80L mutant (right) in lipids of halobacteria (A), bR reconstituted in egg PC bilayer at ambient temperature (B) and at −10 °C (C).

left] were examined, although their signals were broadened compared with those of purple membrane (Fig. 7, top trace).

It is also notable that a reduced lipid–protein interaction achieved by diluting the polar lipids with neutral lipids as under the present experimental conditions is preferable for observation of better ^{13}C NMR signals from [1-^{13}C]Val-bR [Figures 13(A) and (B), left]. This may be the reason why better ^{13}C NMR spectra were obtained for *p*pR expressed in *E. coli* which lacks polar lipids. It is worthwhile, however, examining the conditions for recording full ^{13}C NMR signals under the condition of a 2D array *in the presence* of such polar lipids at low temperatures. Such a study is under way. Of course, it is also possible to modify the time-scale to suppress peaks by means of fast spinning experiments, for instance.

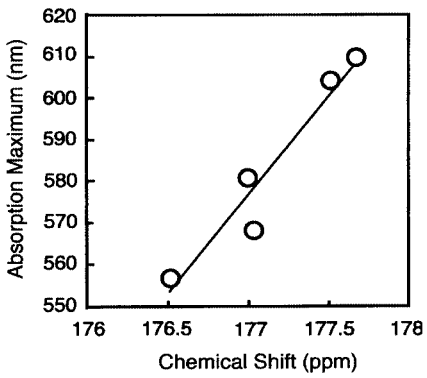

Figure 13. Plot of the UV absorption maximum vs ^{13}C chemical shifts of the Val-213 peak for a variety of mutants used.

Perspective

We have found that dynamic aspect of membrane proteins is strongly dependent on the type of amino acid residues, as viewed from the ^{13}C NMR spectral features of residues located at the surface. So far, we have accomplished the assignment of up to 60 and 70% of the ^{13}C NMR peaks for [3-^{13}C]Ala- and [1-^{13}C]Val-labeled bR, respectively, together with three assigned [1-^{13}C]Pro peaks for residues located at kinked positions[34] and some Trp and Ile signals as mentioned above. Obviously, the present site-directed ^{13}C NMR approach has proved to be a very useful means to examine the local conformation and dynamics of any given membrane protein in view of the observed spectral changes, either displacement or suppression of peaks depending on the conformational and dynamics changes, respectively, at individual residues provided that their ^{13}C NMR signals are properly assigned in the manner mentioned above. In particular, we have now demonstrated that all the ^{13}C NMR signals of [1-^{13}C]Val-labeled residues located at the interhelical loops, Val-34 (A–B loop), −101 (C–D loop), -130 (D–E loop) and -199 (F–G loop) can be distinguished and served as very convenient probes to examine global conformational changes in bR induced by introduced mutations at specific locations, in contrast to the cases of [1-^{13}C]Ala residues in which all the ^{13}C NMR signals from such a region were suppressed. In particular, we found that the M-like state of D85N mutant achieved at pH 10 results in a major conformational change at the extracellular side, as demonstrated by appreciable spectral changes in these loop regions.[45]

Surprisingly, it turned out that Val-151 located near the cytoplasmic end of the helix E undergoes very flexible

motions, as characterized by shortened spin–lattice relaxation times, and can be recorded in the DD/MAS spectra irrespective of the location at the transmembrane α-helix. It is emphasized that this kind of information about protein dynamics cannot be obtained by diffraction data in which such motion, if any, could be frozen at low temperatures to be examined by the diffraction method. In a similar manner, we have demonstrated that the ^{13}C NMR peak of [3-^{13}C]Ala-labeled Ala-184 in the helix F resonates at an unusually low peak position because of the presence of a kinked structure at ambient temperature due to Pro-186.[18] Naturally, we found that such a low-field peak of Ala-184 is absent in the P186A mutant in which this kind of kinked structure is no longer present.[18]

Finally, we emphasize that the ^{13}C NMR peak of Val-213 located at a retinal pocket is well related to the UV absorption maximum demonstrated in Fig. 13. Theoretically the ^{13}C chemical shift of the carbonyl carbon varies with both the torsion angles at the peptide unit and the manner of hydrogen bonding.[45] Therefore, the presence of the low-field peak at 177.0 ppm in bR is caused by strong hydrogen bond interactions in view of the similarity of the torsion angles of the α-helix. In fact, Val-213 of bR participates in bifurcated three-centered hydrogen bonds with Val-217 (with a hydrogen bond length of 2.81 Å) and Gly-218 (2.78 A).[46] It appears that this kind of correlation can be utilized in relation to color tuning in *p*pR.

CONCLUSION

We have found that the site-directed ^{13}C NMR approach is a very powerful means to reveal the conformation and dynamics of *fully hydrated, intact* membrane proteins at ambient temperature, provided that the ^{13}C NMR signals of appropriate ^{13}C-labeled amino acid residues are well resolved and assigned site specifically. This is because several ^{13}C NMR signals from residues near the membrane surfaces in bR from purple membrane (2D crystals) could be suppressed when the frequency of local backbone fluctuation motion, if any, is very close to the proton decoupling frequency or frequency of magic angle spinning. In this connection, it is recommended to utilize [1-^{13}C]Val- or -Ile-bR, and also [3-^{13}C]Ala-labeled protein, as the most appropriate choice as viewed from the least interference mentioned above. This is the reason why detailed assignments of the ^{13}C NMR peaks for these systems are desirable as in the case of [1-^{13}C]Val residues (over 60%). Further, we found that ^{13}C NMR signals from the loops and some transmembrane α-helices of [3-^{13}C]Ala are usually suppressed at ambient temperature when reconstituted membrane proteins taking monomeric form were utilized. Under such a condition, it should be noted that several ^{13}C NMR signals might be suppressed and further experiments to prevent such interference are necessary by changing the experimental conditions toward formation of a 2D array at low temperatures in the presence of annular lipids, or reducing lipid–protein interactions to remove such lipids, or measurement at high temperature, etc.

Acknowledgements

We thank Professor Mikio Kataoka of Nara Institute of Advanced Science and Technology for providing I222C mutant. This work was supported, in part, by a Grant-in-Aid for Scientific Research from the Ministry of Education, Science, Culture and Sports of Japan.

REFERENCES

1. Branden C, Tooze J. *Introduction to Protein Structure* (2nd edn). Garland Publising: New York, 1999.
2. Yamaguchi S, Tuzi S, Yonebayashi K, Naito A, Needleman R, Lanyi JK, Saitô H. *J. Biochem. (Tokyo)* 2001; **129**: 373.
3. Pauli J, Baldus M, van Rossum B, de Groot H, Oschkinart H. *ChemBioChem.* 2001; **2**: 272.
4. Detken A, Hardy EH, Ernst M, Kainosho M, Kawakami T, Aimoto S, Meier BH. *J. Biomol. NMR* 2001; **20**: 203.
5. Saitô H, Tuzi S, Yamaguchi S, Tanio M, Naito A. *Biochim. Biophys. Acta* 2000; **1460**: 39.
6. Saitô H, Tuzi S, Tanio M, Naito A. *Annu. Rep. NMR Spectrosc.* 2002; **47**: 39.
7. Saitô H. *Magn. Reson. Chem.* 1986; **24**: 835.
8. Saitô H, Ando I. *Annu. Rep. NMR Spectrosc.* 1989; **21**: 209.
9. Saitô H, Tuzi S, Naito A. *Annu. Rep. NMR Spectrosc.* 1998; **36**: 79.
10. Tuzi S, Naito A, Saitô H. *Eur. J. Biochem.* 1996; **239**: 294.
11. Blaurock AE, Stoeckenius W. *Nat. New Biol.* 1971; **2**: 152.
12. Tuzi S, Naito A, Saitô H. *Biochemistry* 1994; **33**: 15 046.
13. Yamaguchi S, Tuzi S, Seki T, Tanio M, Needleman R, Lanyi JK, Naito A, Saitô H. *J. Biochem. (Tokyo)* 1998; **123**: 78.
14. Tuzi S, Naito A, Saitô H. *Eur. J. Biochem.* 1993; **218**: 837.
15. Tuzi S, Naito A, Saitô H. *Eur. J. Biochem.* 1996; **239**: 294.
16. Yamaguchi S, Yonebayashi K, Konishi H, Tuzi S, Naito A, Lanyi JK, Needleman R, Saitô H. *Eur. J. Biochem.* 2001; **268**: 2218.
17. Yonebayashi K, Yamaguchi S, Tuzi S, Saitô H. *Eur. Biophys. J.* 2003; **32**: 1.
18. Tuzi S, Yamaguchi S, Tanio M, Konishi H, Inoue S, Naito A, Needleman R, Lanyi JK, Saitô H. *Biophys. J.* 1999; **76**: 1523.
19. Tuzi S, Hasegawa J, Kawaminami R, Naito A, Saitô H. *Biophys. J.* 2001; **81**: 425.
20. Tanio M, Inoue S, Yokota K, Seki T, Tuzi S, Needleman R, Lanyi JK, Naito A, Saitô H. *Biophys. J.* 1999; **77**: 431.
21. Tanio M, Tuzi S, Yamaguchi S, Kawaminami R, Naito A, Needleman R, Lanyi JK, Saitô H. *Biophys. J.* 1999; **77**: 1577.
22. Saitô H, Kawaminami R, Tanio M, Arakawa T, Yamaguchi S, Tuzi S. *Spectroscopy* 2002; **16**: 107.
23. Kawase Y, Tanio M, Kira A, Yamaguchi S, Tuzi S, Naito A, Kataoka M, Lanyi JK, Needleman R, Saitô H. *Biochemistry* 2000; **39**: 14 472.
24. Saitô H, Tsuchida T, Ogawa K, Arakawa T, Yamaguchi S, Tuzi S. *Biochim. Biophys. Acta* 2002; **1565**: 97.
25. Arakawa T, Shimono K, Yamaguchi S, Tuzi S, Sudo Y, Kamo N, Saitô H. *FEBS Lett.* 2003; **536**: 237.
26. Suwelack D, Rothwell WP, Waugh JS. *J. Chem. Phys.* 1980; **73**: 2559.
27. Rothwell WP, Waugh JS. *J. Chem. Phys.* 1981; **74**: 2721.
28. Yamaguchi S, Tuzi S, Tanio M, Naito A, Lanyi JK, Needleman R, Saitô H. *J. Biochem. (Tokyo)* 2000; **127**: 861.
29. Solomon I. *Phys. Rev.* 1955; **99**: 559.
30. Bloembergen N. *J. Chem. Phys.* 1957; **27**: 572.
31. Needleman R, Chang M, Ni B, Varo G, Fornes J, White SH, Lanyi JK. *J. Biol. Chem.* 1991; **266**: 11 478.
32. Onishi H, McCance EM, Gibbons NE. *Can. J. Microbiol.* 1965; **11**: 365.
33. Oesterhelt D, Stoeckenius W. *Proc. Natl. Acad. Sci. USA* 1973; **70**: 2853.
34. Tuzi S, Naito A, Saitô H. *J. Mol. Struct.* 2003; **654**: 205.
35. Kamihira M, Naito A, Nishimura K, Tuzi S, Saitô H. *J. Phys. Chem. B* 1998; **102**: 2826.
36. Kamihira M, Naito A, Tuzi S, Saitô H. *J. Phys. Chem. A* 1999; **103**: 3356.
37. Saitô H, Yamaguchi S, Okuda H, Shiraisi A, Tuzi S. *Solid State NMR Spectrosc.* 2003; in press.

38. Krebs MP, Isenberger TA. *Biochim. Biophys. Acta* 2000; **1460**: 15.
39. Saitô H, Yamamoto K, Tuzi S, Yamaguchi S. *Biochim. Biophys. Acta* 2003; in press.
40. Sternberg B, Gale P, Watts A. *Biochim. Biophys. Acta* 1989; **980**: 117.
41. Sternberg B, L'Hostis C, Whiteway CA, Watts A. *Biochim. Biophys. Acta* 1992; **1108**: 21.
42. Watts A. *Biophys. Chem.* 1995; **55**: 137.
43. Sabra MC, Utidehaag JCM, Watts A. *Biophys. J.* 1998; **75**: 1180.
44. Kira A, Tanio M, Tuzi S, Saitô H. *Eur. Biophys. J.* submitted.
45. Ando I, Saitô H, Tabeta R, Shoji A. *Macromolecules* 1984; **17**: 457.
46. Luecke H, Schobert B, Richter HT, Cartailer JP, Lanyi JK. *J. Mol. Biol.* 1999; **291**: 899.